arXiv:2608.13602v1 [cs.MM] 7 Aug 2026

Omni-LiveAvatar: Minute-Level Real-Time Streaming Joint Audio-Visual Avatar Generation

Lunjie Zhu[1,2], Xingtong Ge[1,2], Fangyu Lin[1,2], Yi Zhang[2], Zhening Liu[1], Mengfei Li[1,2], Yumeng Zhang[1], Guanglu Song[2], Yu Liu[2], Jun Zhang[1*]

[1]iComAI Lab, Hong Kong University of Science and Technology
[2]Vivix Group Limited
lzhubb@connect.ust.hk, eejzhang@ust.hk

Abstract

Joint audio-video generative models serve as foundation for immersive and interactive digital-human generation. Nevertheless, most existing models rely on bidirectional attention and multi-step denoising and can generate only short clips, making them unsuitable for real-time interaction over extended durations. We present **Omni-LiveAvatar**, the first framework for minute-level, real-time streaming joint audio-video avatar generation. Specifically, we propose (1) a *progressive autoregressive distillation pipeline* that transfers a large bidirectional joint audio-video diffusion model into a few-step autoregressive generator without auxiliary stabilization mechanisms; (2) a *synchronized audio-video long-short-term memory* that preserves global consistency under a bounded memory budget; and (3) a *hierarchical rolling prompt planning* strategy that enables coherent semantic evolution and seamless prompt transitions. Extensive experiments show that Omni-LiveAvatar generates high-quality, synchronized minute-level avatars in real time. In terms of speed, it achieves a **33**× generation speedup over its teacher, LTX-2, on a single NVIDIA H200 GPU; in terms of generation quality, it outperforms accelerated baselines across visual quality, audio quality, cross-modal synchronization, and human fidelity. Our code is available at https://github.com/Aoko955/Omni-LiveAvatar

1 Introduction

Recently, remarkable progress has been made in joint audio-video generative models (HaCohen et al. 2026; Low, Wang, and Katyal 2025) for synthesizing high-fidelity, synchronized multimodal content. These advances lay a strong foundation for interactive digital-human applications that demand realistic appearance, coherent motion, and accurate lip-synced speech (Lin et al. 2026). However, most existing models rely on bidirectional attention and multi-step denoising, which incurs high inference latency and confines generation to short clips. This makes them unsuitable for latency-sensitive applications that require continuous interaction over extended durations.

To enable real-time streaming generation, recent works (Su et al. 2026; Li et al. 2026) adapt autoregressive distillation techniques (Ge et al. 2026a,b) originally developed for video generation to joint audio-video models. However, these methods largely rely on modality-specific remedies, such as audio sink tokens or additional future audio context, and external components such as reward models. While effective, they do not examine whether the classic distillation pipeline remains suitable for joint generation given the increased model scale and the inherent complexity of multimodal modeling. Moreover, existing joint audio-video autoregressive distillation methods are primarily restricted to short-clip generation, leaving stable minute-level streaming avatar generation underexplored.

To address these challenges, we present **Omni-LiveAvatar**, the first framework for minute-level, real-time streaming joint audio-video avatar generation. Rather than patching an unstable training pipeline with modality-specific remedies, we revisit the classic distillation pipeline at a more fundamental level and develop a *progressive autoregressive distillation* pipeline that converts a bidirectional teacher into a real-time streaming generator without auxiliary designs. For minute-level generation, we introduce a *synchronized audio-video long-short-term memory* mechanism that combines periodically re-anchored long-term memory with a rolling key-value (KV) cache, preserving global consistency and recent context under a bounded memory budget. To schedule long prompts under the joint audio-video rolling-forcing (Liu et al. 2025b) setting without semantic conflicts across prompt transitions, we propose a *hierarchical rolling prompt planning* strategy that decomposes the full prompt into a fixed global prompt, which specifies persistent appearance, background, and overall motion, as well as block-level local prompts that advance together with the rolling window, thereby avoiding the overlapping or blurred speech caused by abrupt prompt switching.

In summary, our work focuses on real-time, long-duration joint audio-video avatar synthesis and makes the following contributions:

- We propose a progressive autoregressive distillation pipeline that transfers a large bidirectional audio-video diffusion model into a few-step causal generator without auxiliary stabilization mechanisms.
- We design a synchronized audio-video long-short-term memory mechanism that sustains global consistency and cross-modal alignment under a bounded memory budget.
- We introduce a hierarchical rolling prompt planning strategy that enables coherent semantic transitions under the joint rolling-forcing setting.

*Corresponding author.

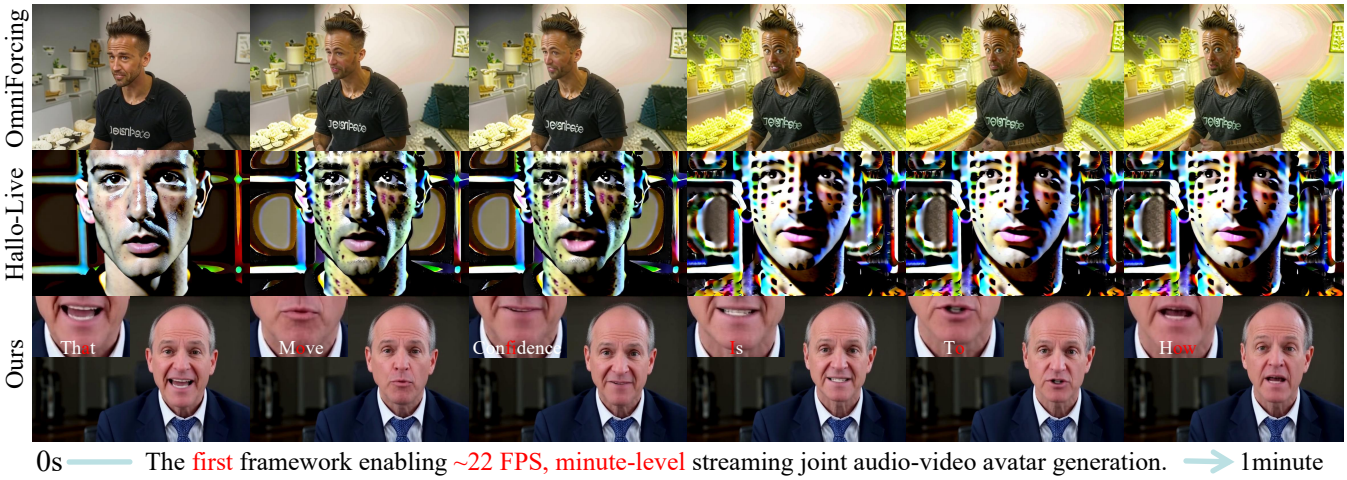

Figure 1: Qualitative comparison of minute-level generation. Compared with state-of-the-art baselines, Omni-LiveAvatar preserves consistent avatar and background appearance, and maintains tight audio-video alignment over a minute-long rollout, whereas OmniForcing and Hallo-Live exhibit severe appearance drift. In the bottom row, the syllable uttered at each frame is highlighted in red, and the insets show the corresponding mouth shapes for lip-audio alignment.

- Extensive experiments show that Omni-LiveAvatar generates high-quality, synchronized minute-level audio-video avatars in real time, achieving a **33**× generation speedup over its teacher LTX-2 while outperforming accelerated baselines across all evaluated dimensions.

2 Related Work

Audio-Driven Avatar Generation. Building on powerful diffusion models (Wan et al. 2025; Kong et al. 2024), audio-driven avatar generation has witnessed remarkable advances in visual fidelity (Tian et al. 2024; Xu et al. 2024a; Chen et al. 2024; Cui et al. 2025; Chen et al. 2025), long-duration consistency (Jiang et al. 2025; Cui et al. 2024; Yang et al. 2025b; Tu et al. 2025), and real-time streaming capability (Xu et al. 2024b; Zhen et al. 2025; Huang et al. 2026c; Shen et al. 2025). However, these audio-driven methods rely on pre-generated audios and lack mutual adaptation between the audio and video streams, complicating the overall generation pipeline and limiting flexible audio-video coordination.

Autoregressive Joint Audio-Video Generation. Joint audio-video generation models produce both audio and video within a unified framework and generally follow three paradigms: cascaded generation (Ruan et al. 2023), dual-stream modeling with cross-modal interaction (Low, Wang, and Katyal 2025; HaCohen et al. 2026), and unified single-stream modeling (SII-GAIR et al. 2026). However, they all rely on bidirectional attention and multi-step denoising, resulting in slow inference and high computational costs (Low, Wang, and Katyal 2025; HaCohen et al. 2026; Li et al. 2025; Huang et al. 2026a,b).

To enable real-time interactive applications, recent works adapt autoregressive distillation pipelines and acceleration techniques (Yin et al. 2025; Huang et al. 2025; Zhu et al. 2026) developed for video models to joint audio-video models. OmniForcing (Su et al. 2026) introduces audio sink tokens to stabilize joint audio-video causalization, while Hallo-Live (Li et al. 2026) employs future-expanding audio attention and preference-guided distribution matching distillation (DMD) with external reward models. However, these approaches address the challenges of joint audio-video autoregressive distillation mainly through auxiliary stabilization mechanisms or external supervision, rather than fundamentally revisiting the distillation framework. Moreover, existing methods are designed and evaluated primarily for short-clip generation, leaving stable minute-level generation underexplored.

3 Method

3.1 Problem Formulation and Method Overview

Given a text prompt $\mathcal{C}$ describing an avatar, scene, and audio content, our goal is to generate a minute-level avatar video $\mathbf{V}$ together with synchronized audio $\mathbf{A}$ in real time. While a natural direction is to extend autoregressive distillation methods from video generation to joint audio-video generation, this extension faces three challenges: (i) scaling the distillation to larger multi-modal models, where audio modeling and cross-modal coupling increase distillation difficulty; (ii) controlling cross-modal drift, where visual and audio drifts accumulate over time and reinforce each other, degrading identity consistency, speech quality, and lip synchronization; and (iii) scheduling heterogeneous semantics, to coordinate the slowly varying visual context with rapidly changing speech content over minute-long generation. Omni-LiveAvatar addresses these challenges with progressive autoregressive distillation, synchronized audio-video long-short-term memory, and hierarchical rolling prompt planning, whose details are presented in the following subsections.

3.2 Progressive Autoregressive Distillation for Joint Audio-Visual Generation

Existing autoregressive distillation methods for video generation (Liu et al. 2025b; Huang et al. 2025) typically initialize

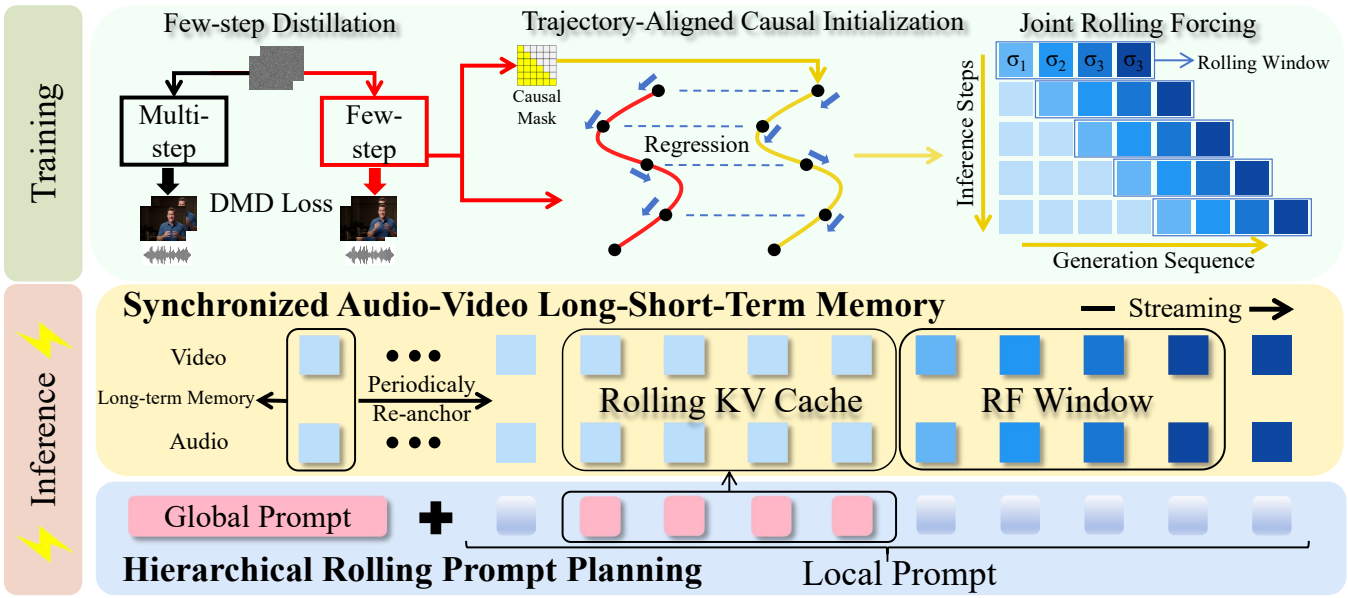

Figure 2: Overview of Omni-LiveAvatar. The proposed progressive autoregressive distillation pipeline converts a large bidirectional audio-video diffusion model into a few-step causal generator without any auxiliary stabilization mechanism (top). At inference, the synchronized audio-video long-short-term memory preserves global consistency while retaining recent context within a bounded memory budget for minute-level streaming inference (middle), and the hierarchical rolling prompt planning organizes global and local prompts for smooth long-form semantic evolution (bottom).

a few-step causal student by regressing the ordinary differential equation (ODE) trajectories of a pre-trianed bidirectional teacher. However, such initialization does not readily extend to joint audio-video generation, where the larger model scale, complex cross-modal coupling, and modality asymmetry make bidirectional-to-causal adaptation substantially more difficult. To obtain a stronger few-step causal initialization, OmniForcing (Su et al. 2026) decouples few-step distillation from causal adaptation by first applying distribution matching distillation (DMD) to obtain a lightweight few-step generator and then performing causal ODE regression. However, its ODE pairs are generated by the original multi-step teacher[1]. As illustrated in Figure 3, DMD matches the output distribution but does not preserve the pointwise denoising trajectory. Therefore, the causal student is forced to regress toward ODE targets from a different trajectory, which leads to unstable causal training and explains why OmniForcing requires additional stabilization mechanisms.

To address these issues, we develop a progressive autoregressive distillation pipeline comprising few-step distillation, trajectory-aligned causal initialization, and joint rolling forcing, enabling stable causal adaptation and efficient few-step generation without relying on auxiliary designs. Specifically, in Stage I, we first distill the pretrained bidirectional audio-video diffusion model $G^{\text{bi}}_{\text{base}}$ into a bidirectional few-step generator $G^{\text{bi}}_{\text{few}}$, optimizing the student with a joint audio-video DMD loss (Yin et al. 2024):

$$\mathcal{L}_{\text{Bi-DMD}} = \lambda_v \mathcal{L}^v_{\text{DMD}} + \lambda_a \mathcal{L}^a_{\text{DMD}}, \tag{1}$$

where λ_v and λ_a balance the video and audio losses.

[1]https://github.com/OmniForcing/OmniForcing/issues/8

In Stage II, we convert $G^{\text{bi}}_{\text{few}}$ into a causal few-step generator $G^{\text{causal}}_{\text{few}}$ by applying a block-causal attention mask over audio-video macro-blocks, where $B_k = (V_k, A_k)$ denotes the k-th macro-block containing temporally aligned video and audio latents over a one-second interval (Su et al. 2026). To avoid trajectory mismatch and stabilize causal initialization, we generate ODE pairs with the frozen $G^{\text{bi}}_{\text{few}}$ and train $G^{\text{causal}}_{\text{few}}$ via ODE regression:

$$\begin{aligned}\mathcal{L}_{\text{C-ODE}} =& \lambda_v \left\| v^v_\theta(\mathbf{x}_t) - v^v_\phi(\mathbf{x}_t) \right\|_2^2 \\ &+ \lambda_a \left\| v^a_\theta(\mathbf{x}_t) - v^a_\phi(\mathbf{x}_t) \right\|_2^2,\end{aligned} \tag{2}$$

where $\mathbf{x}_t$ is the joint noisy latent at denoising timestep t, v_ϕ and v_θ denote the velocity predictions of the bidirectional few-step teacher $G^{\text{bi}}_{\text{few}}$ and the causal student $G^{\text{causal}}_{\text{few}}$ at $\mathbf{x}_t$, respectively. λ_v and λ_a balance the video and audio regression losses.

However, strict block-causal rollout causes errors to propagate and accumulate unidirectionally, leading to severe drift during long-horizon inference. To address this, in Stage III, we introduce joint rolling forcing. Specifically, we construct a rolling window of M consecutive macro-blocks with progressively increasing noise levels:

$$\mathcal{W}_k = \{B^{\sigma_1}_k, B^{\sigma_2}_{k+1}, \ldots, B^{\sigma_M}_{k+M-1}\},\ \sigma_1 < \cdots < \sigma_M. \tag{3}$$

where B^σ_i denotes the i-th audio-video macro-block at noise level σ. In each forward pass, all blocks inside $\mathcal{W}_k$ are jointly denoised with bidirectional intra-modal and cross-modal attention within the window. The cleanest block, $B^{\sigma_1}_k$, then exits the window, while the remaining blocks advance to the next denoising step with a new Gaussian-noise-corrupted

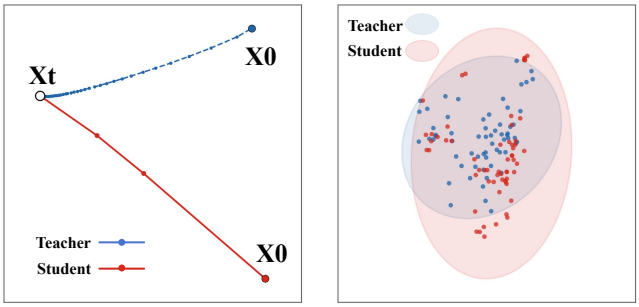

Figure 3: Visualization of the denoising trajectories (left) and output distributions (right) of the multi-step teacher and few-step student. Projected via principal component analysis, the visualization shows that DMD aligns the output distribution but disrupts the pointwise denoising trajectory.

block being appended. We train this stage with the same joint audio-video DMD objective as in Stage I, applied over all macro-blocks in $\mathcal{W}_k$.

Because the active rolling window enables bidirectional interaction, earlier blocks are no longer frozen as potentially erroneous context for later blocks. Instead, they can leverage information from future blocks for refinement, thereby suppressing unidirectional error propagation. Moreover, audio latents form a one-dimensional temporal sequence and are easier to model than high-dimensional video latents, thus granting the video branch access to future audio cues therefore improves both the visual quality and cross-modal alignment.

3.3 Synchronized Audio-Video Long-Short-Term Memory

Existing streaming joint audio-video avatar generators (Li et al. 2026) primarily rely on KV caches (Zhao et al. 2025) to preserve recent context during causal inference. Although a rolling KV cache can propagate visual and voice information across adjacent blocks, these attributes are inherited recursively from imperfect model predictions, so small deviations may accumulate over long horizons and eventually cause drift.

To counteract this drift, we introduce a synchronized audio-video long-short-term memory. We retain the KV states of the first audio-video macro-block $B_0 = (V_0, A_0)$ as long-term memory $\mathcal{M}_{\text{long}}$, which remains permanently visible to all subsequent blocks and provides a stable reference for identity, scene, voice timbre, and audio-video correspondence. In parallel, we maintain a rolling KV cache over the most recent L macro-blocks as short-term memory $\mathcal{M}_{\text{short}}$, which preserves motion and speech continuity. Given access to temporally aligned audio and video states, both memories achieve modality stability through self-attention and cross-modal fidelity through cross-attention.

As generation proceeds, the relative positional offset between the long-term memory and current queries increases, weakening the influence of the long-term memory embedded in the Rotary Position Embedding (RoPE). To address this problem, we periodically re-anchor the long-term memory. Specifically, We store its pre-RoPE keys $\mathbf{K}^{\text{orig}}$ and, after each five-second chunk has been generated, reapply RoPE to $\mathbf{K}^{\text{orig}}$ using positions immediately preceding the current rolling KV cache while keeping the corresponding values unchanged. This preserves the memory content while reducing the RoPE position gap between the long-term memory and current queries, maintaining the influence of the long-term memory during minute-level generation.

3.4 Hierarchical Rolling Prompt Planning

With progressive autoregressive distillation and synchronized audio-video long-short-term memory, OmniLiveAvatar achieves stable real-time inference for long-horizon joint generation. However, the joint rolling-forcing paradigm introduces two new challenges for prompt planning. First, fixed-interval prompt switching, as adopted in LongLive (Yang et al. 2025a), is incompatible with rolling forcing: when a rolling window crosses a prompt boundary, blocks conditioned on different prompts are jointly denoised and attend to each other, causing semantic conflicts and leading to overlapping or blurred speech near transitions. Second, audio and video require textual conditioning at different temporal granularities. Visual semantics such as identity, scene, and motion evolve slowly and are better controlled by coarse-grained prompts, whereas speech content changes continuously and requires fine-grained sentence-level updates.

To address these challenges, we propose a hierarchical rolling prompt planning strategy. Specifically, we decompose the full prompt into a global prompt for persistent sequence-level semantics and local prompts for block-level speech content. For the global prompt $\mathcal{P}^{\text{global}}$, we keep its embedding fixed throughout generation, providing a stable global condition. For the local prompts, we partition the speech description into block-level segments, where $\mathcal{P}_k^{\text{local}}$ denotes the local prompt assigned to macro-block B_k. For each rolling window $\mathcal{W}_k$, the effective condition is formed by concatenating the fixed global prompt with the local prompts of the blocks within the rolling window:

$$\mathcal{P}(\mathcal{W}_k) = \left[\mathcal{P}^{\text{global}};\, \mathcal{P}_k^{\text{local}}, \ldots, \mathcal{P}_{k+M-1}^{\text{local}}\right]. \tag{4}$$

When the rolling window advances from $\mathcal{W}_k$ to $\mathcal{W}_{k+1}$, the oldest local prompt $\mathcal{P}_k^{\text{local}}$ leaves the window and the local prompt $\mathcal{P}_{k+M}^{\text{local}}$ of the newly entering block is appended, so the effective condition shifts smoothly rather than switching abruptly at fixed boundaries. Together, the hierarchical rolling prompt planning enables smooth scheduling of textual conditions at different granularities under the joint rolling-forcing paradigm.

4 Experiments

In this section, we first describe the experimental setup, including the baselines, implementation details, and evaluation protocols in Section 4.1. We then present the main results of the generation quality and speed for both 5-second and minute-level streaming generation in Section 4.2. Finally, we conduct ablation studies to validate the design choices of key components in Section 4.3.

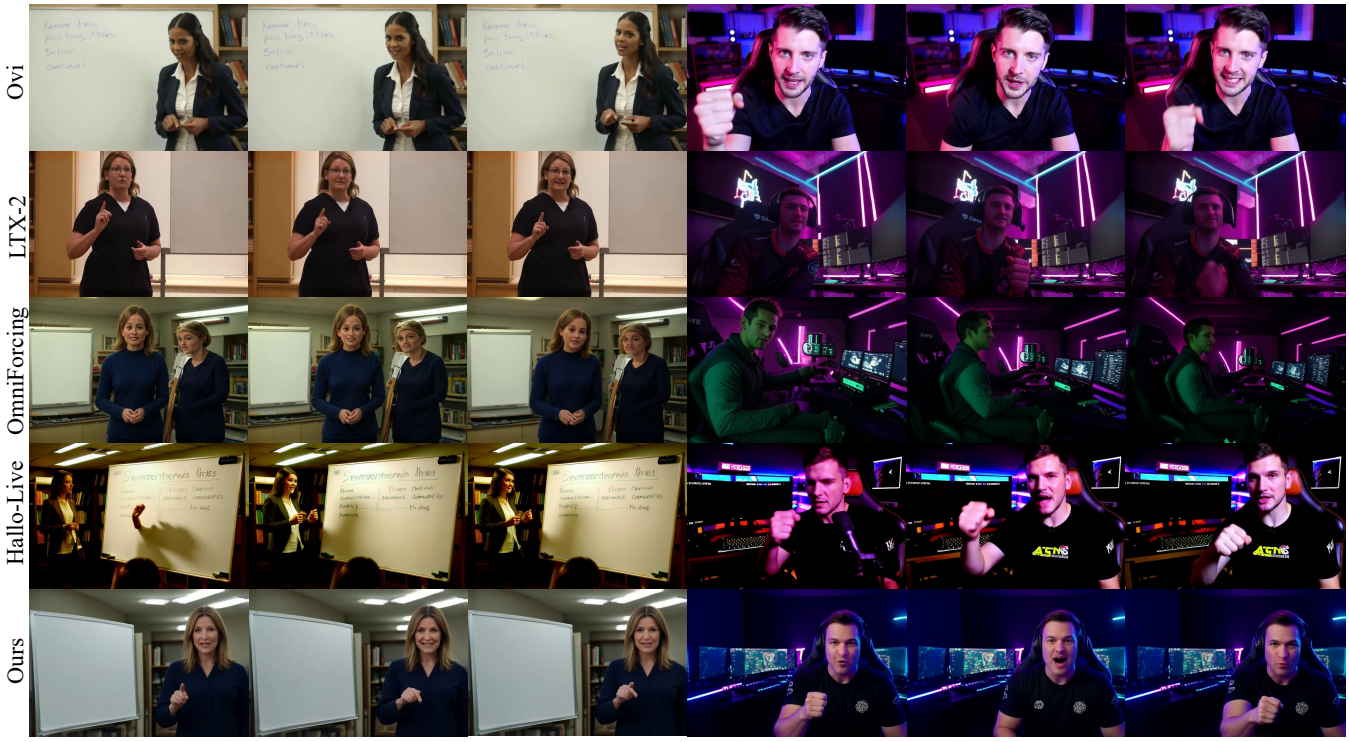

Figure 4: Qualitative comparison of 5-second avatar generation. Omni-LiveAvatar generates realistic and temporally consistent avatars with visual quality comparable to Ovi and LTX-2, whereas OmniForcing exhibits noticeable realism degradation and Hallo-Live suffers from facial and hand artifacts as well as color drift.

4.1 Experimental Setup

Baselines. We compare Omni-LiveAvatar against two representative frameworks for real-time autoregressive joint audio-video generation:

- **OmniForcing** (Su et al. 2026): the current state-of-the-art (SOTA) framework for general text-to-audio-video (T2AV) generation.
- **Hallo-Live** (Li et al. 2026): the current SOTA framework for avatar-specific audio-video generation.

Metrics. To comprehensively evaluate Omni-LiveAvatar, we compare model capabilities across six dimensions: video quality, text-video alignment, human fidelity, audio quality, audio-video alignment, and generation speed.

For video quality (VQ), we use VBench (Huang et al. 2023) to evaluate per-frame fidelity and temporal coherence, reporting the Quality Score (QS) together with Subject Consistency (SC), Background Consistency (BC), Aesthetic Quality (AQ), and Imaging Quality (IQ). For long-form video quality, we use VBench-Long (Huang et al. 2024) and report Subject Consistency (SC), Motion Smoothness (MS), Aesthetic Quality (AQ), and Imaging Quality (IQ). For text-video alignment, we use VideoAlign (VA) (Liu et al. 2025a) to assess semantic consistency between the generated video and the text prompt. For text-video alignment, we use VideoAlign (VA) (Liu et al. 2025a). For human fidelity, we adopt human-centric metrics from VBench 2.0 (Zheng et al. 2025) to evaluate the quality and consistency of generated avatars, including Human Anatomy (HA), Human Identity (HI), and Human Clothing (HC). For audio quality, we report three non-intrusive mean opinion score (MOS) predictors commonly used in speech synthesis and speech quality assessment: UTMOS (Saeki et al. 2022) (UT) for speech naturalness, DNSMOS (Reddy, Gopal, and Cutler 2022) (DN) for noise and distortion, and NISQA (Mittag et al. 2021) (NI) for temporal continuity. For audio-video alignment, we use SyncNet confidence (Chung and Zisserman 2016) (Sync-C) to measure lip-speech synchronization. For generation speed, we follow Rolling Forcing (Liu et al. 2025b) and report throughput in frames per second (FPS) on a single NVIDIA H200 GPU to quantify real-time streaming capability.

Implementation Details. We build Omni-LiveAvatar on top of the 19B LTX-2 model (HaCohen et al. 2026). All training is conducted on 8 NVIDIA H200 GPUs in bf16 precision using the AdamW optimizer with a global batch size of 8. We train Omni-LiveAvatar on an internal dataset of 35K text prompts. Using these prompts, we generate the Stage II ODE regression pairs from our Stage-I few-step model. We train Stage I, Stage II, and Stage III for 4,000, 3,000, and 3,000 steps, with learning rates of 2×10^{-5}, 1×10^{-4}, and 2×10^{-5}, respectively. For the training objective, the video and audio losses are equally weighted ($\lambda_v = \lambda_a = 1.0$) across all stages, and the classifier-free guidance scales in the DMD stages (Stage I and Stage III) are set to 3 and 5 for the video and audio streams, respectively. For the memory con-

Method	Speed	Video Quality					VA↑	Human Fidelity			Audio Quality			Sync-C↑
	FPS↑	SC↑	BC↑	AQ↑	IQ↑	QS↑		HA↑	HI↑	HC↑	UT↑	DN↑	NI↑	
Bidirectional Models														
LTX-2 (HaCohen et al. 2026)	0.60	92.54	93.42	56.37	71.53	79.39	7.77	96.23	92.93	99.57	3.54	3.75	3.47	6.89
Ovi (Low, Wang, and Katyal 2025)	1.41	97.10	95.29	33.13	65.83	76.14	6.51	98.55	97.13	99.19	3.10	3.72	2.63	6.88
Real-time Autoregressive Models														
OmniForcing (Su et al. 2026)	16.11	98.05	94.47	60.14	70.75	80.05	8.11	88.76	98.51	**100.00**	2.46	3.84	3.03	1.60
Hallo-Live (Li et al. 2026)	16.50	98.20	93.64	27.97	66.04	74.21	8.04	98.39	97.42	**100.00**	2.96	3.81	2.95	4.50
Omni-LiveAvatar	**19.57**	**99.28**	**97.52**	**63.61**	**72.11**	**81.72**	**9.08**	**98.76**	**100.00**	**100.00**	**3.19**	**3.95**	**3.06**	**6.16**

Table 1: Quantitative comparison on 5-second avatar generation. The best results among the real-time autoregressive models are highlighted in bold, and ↑ indicates that higher values are better.

Method	Speed	Video Quality				VA↑	Human Fidelity			Audio Quality			Sync-C↑
	FPS↑	SC↑	MS↑	AQ↑	IQ↑		HA↑	HI↑	HC↑	UT↑	DN↑	NI↑	
Real-time Autoregressive Models													
OmniForcing (Su et al. 2026)	16.18	98.71	99.38	54.90	71.70	6.68	92.14	50.19	**100.00**	1.60	3.51	2.90	0.28
Hallo-Live (Li et al. 2026)	13.80	99.50	99.19	47.16	61.18	5.46	97.81	67.60	77.20	2.02	3.97	2.99	0.72
Omni-LiveAvatar	**21.99**	**99.55**	**99.68**	**61.98**	**71.71**	**9.82**	**99.85**	**98.61**	**100.00**	**2.80**	**4.04**	**3.24**	**6.76**

Table 2: Quantitative comparison on minute-level avatar generation. Omni-LiveAvatar achieves the best performance across all evaluated metrics, with particularly strong speed, aesthetic quality (AQ), human identity (HI) fidelity, and audio-video alignment.

figuration, both the rolling-forcing window and the rolling KV cache span 4 macro-blocks, while the long-term memory retains the first macro-block. During inference, our few-step generator produces each block in four denoising steps at a resolution of 512×768, enabling streaming generation up to minute-level duration.

4.2 Main Results

We compare Omni-LiveAvatar against two families of baselines: offline bidirectional joint audio-video generation models, including LTX-2 (HaCohen et al. 2026) and Ovi (Low, Wang, and Katyal 2025), and real-time autoregressive distilled models, including OmniForcing (Su et al. 2026) and Hallo-Live (Li et al. 2026). We conduct comprehensive experiments on both 5-second and 60-second sequence generation, demonstrating that Omni-LiveAvatar outperforms the autoregressive distilled baselines in both short-clip and long-sequence generation.

Generation Results on 5-Second Clips. We present the quantitative and qualitative results in Table 1 and Figure 4, respectively. As shown in Figure 4, OmniForcing (Su et al. 2026) produces avatars with degraded realism and Hallo-Live (Li et al. 2026) suffers from facial artifacts, spurious hands, and noticeable color bias and drift. In contrast, Omni-LiveAvatar generates natural and consistent avatars, achieving visual quality comparable to the two bidirectional models. Quantitatively, Omni-LiveAvatar achieves real-time generation at 19.57 FPS on a single NVIDIA H200 GPU, delivering a $\sim 33\times$ speedup over its bidirectional teacher LTX-2 and a speedup of about $1.2\times$ over the autoregressive distilled baselines. In terms of video quality and human-centric fidelity, Omni-LiveAvatar outperforms all competitors, including both bidirectional and autoregressive models. Its overall quality score (QS) exceeds the second-best result by 1.7 (81.72 vs. 80.05), and its human identity (HI) and clothing (HC) fidelity both reach a perfect score of 100. Omni-LiveAvatar also achieves the best text-video alignment (VA), surpassing the others by at least 0.97 (9.08 vs. 8.11). For audio quality, Omni-LiveAvatar consistently outperforms the autoregressive baselines across all metrics, with only marginal degradation in naturalness (UT) and continuity (NI) compared with the bidirectional teacher. A similar trend is observed for audio-video synchronization (Sync-C). Overall, these results demonstrate that Omni-LiveAvatar achieves real-time generation without sacrificing quality, consistently outperforming real-time baselines across all evaluated metrics while remaining competitive with offline bidirectional models in quality.

Generation Results on 60-Second Sequences. We show the quantitative and qualitative results for minute-level generation in Table 2 and Figure 1, respectively. As shown in Figure 1, both the avatars and the backgrounds generated by OmniForcing and Hallo-Live exhibit drastic color and structural distortions, whereas Omni-LiveAvatar maintains stable and consistent visual appearance throughout the one-minute sequence. To visualize audio-video synchronization at the syllable level, we transcribe the generated speech using Whisper (Radford et al. 2022), obtain syllable timestamps through forced alignment (McAuliffe et al. 2017), and inspect the mouth shapes in the corresponding video frames. Figure 1

shows that the lip motion generated by Omni-LiveAvatar remains closely aligned with the speech throughout the minute-level generation. Quantitatively, Omni-LiveAvatar outperforms the autoregressive-distilled baselines across all evaluated metrics. Specifically, it achieves real-time streaming generation at 21.99 FPS, running $1.36\times$ faster than the second-fastest baseline (16.18 FPS). The quality improvements are particularly notable in human identity (HI, 98.61 vs. 67.60 and 50.19), audio-video synchronization (Sync-C, 6.76 vs. 0.72 and 0.28), and text-video alignment (VA, 9.82 vs. 6.68 and 5.46). These results demonstrate that Omni-LiveAvatar not only excels on short clips but also pioneers real-time, high-fidelity, and temporally coherent streaming generation at the minute scale.

4.3 Ablation Study

Ablation on Training Methods. To validate our proposed progressive autoregressive distillation strategy, we perform ablations on joint rolling forcing (RF) and trajectory-aligned causal initialization (TA-ODE). Specifically, we compare our method against three settings: (1) using joint self forcing instead of joint rolling forcing and generating the ODE pairs with the multi-step teacher (w/o RF & w/o TA-ODE); (2) using joint self forcing instead of joint rolling forcing (w/o RF); and (3) generating the ODE pairs with the multi-step teacher (w/o TA-ODE). As shown in Table 3, the w/o RF & w/o TA-ODE setting degrades drastically across all evaluated quality metrics. Adding either rolling forcing or TA-ODE alone already yields consistent improvements across all metrics over the w/o RF & w/o TA-ODE variant. However, compared with ours, w/o RF mainly degrades audio quality and audio-video synchronization, reducing UTMOS from 3.19 to 1.93 and Sync-C from 6.16 to 4.58, whereas w/o TA-ODE primarily degrades video quality and text-video alignment, with Qulity Score (QS) dropping from 81.72 to 81.25 and VideoAlign (VA) from 9.08 to 8.63. Only when trajectory-aligned causal initialization and joint rolling forcing are combined does the model achieve the best performance, confirming that the two are jointly necessary.

Ablation on Memory Mechanism. To validate our synchronized audio-video long-short-term memory, we compare it against three settings: (1) without the long-term memory (w/o LTM); (2) without periodic RoPE re-anchoring (w/o re-anchor); and (3) with temporally misaligned audio and video long-term memory (async LTM). As shown in Table 4, the video branch is more dependent on the memory mechanism than the audio branch during long-horizon inference, which indicates that video generation is more vulnerable to temporal drift due to its modality complexity. Specifically, w/o LTM causes the largest degradation in both video quality and audio-video synchronization, with Aesthetic Quality dropping from 61.98 to 58.61 and SyncNet confidence from 6.76 to 5.79. Removing re-anchoring mainly weakens the video quality metrics while async LTM primarily harms cross-modal alignment qualified by SyncNet confidence (Sync-C). These results demonstrate that our synchronized audio-video long-short-term memory guarantees the stability and audio-video alignment of long-horizon generation with sophisticated long-term memory and re-anchoring designs.

Variant	VQ	Audio Quality			Sync-C↑	VA↑
	QS↑	UT↑	DN↑	NI↑		
w/o RF & w/o TA-ODE	72.05	1.51	3.21	2.70	1.23	1.24
w/o RF	80.67	1.93	3.38	2.44	4.58	8.09
w/o TA-ODE	81.25	3.14	3.81	2.96	5.98	8.63
Ours	**81.72**	**3.19**	**3.95**	**3.06**	**6.16**	**9.08**

Table 3: Ablation of training strategies.

Variant	Video Quality		Audio Quality			Sync-C↑	VA↑
	AQ↑	IQ↑	UT↑	DN↑	NI↑		
w/o LTM	58.61	71.16	2.79	4.03	3.22	5.79	9.70
w/o re-anchor	61.16	71.43	2.78	4.02	3.23	6.70	9.82
async LTM	61.93	71.69	2.76	4.03	3.21	6.61	9.80
Ours	**61.98**	**71.71**	**2.80**	**4.04**	**3.24**	**6.76**	**9.82**

Table 4: Ablation of memory mechanisms.

Variant	VQ		Audio Quality			Sync-C↑	VA↑
	AQ↑	IQ↑	UT↑	DN↑	NI↑		
w/o rolling prompt	55.74	68.45	1.60	3.28	2.38	4.47	9.72
5 s-interval switching	61.23	71.33	2.65	3.94	3.19	5.11	9.71
Ours	**61.98**	**71.71**	**2.80**	**4.04**	**3.24**	**6.76**	**9.82**

Table 5: Ablation of prompt planning strategies.

Ablation on Prompt Planning Strategy. To validate our hierarchical rolling prompt planning, we compare it against two settings: (1) providing the full prompt to the model at once (w/o rolling prompt); and (2) updating the prompt every 5 s (5 s-interval switching). As shown in Table 5, the audio-related metrics are more sensitive to the prompt planning strategy than the video-related metrics, indicating that audio requires a finer-grained and smoother prompt schedule. Specifically, exerting the full prompt at once yields the largest drops across nearly all metrics, notably including the audio naturalness (UT) from 2.80 to 1.60 and SyncNet confidence (Sync-C) from 6.76 to 4.47. Updating the prompt every 5 s mainly degrades the audio-quality metrics as well as audio-video alignment, with SyncNet confidence (Sync-C) dropping from 6.76 to 5.11. These results show that, under joint rolling-forcing inference paradigm, our hierarchical rolling prompt planning enables smooth, continuous, and aligned audio-video generation

Conclusions

In this paper, we present Omni-LiveAvatar, the first framework for minute-level, real-time streaming joint audio-video avatar generation. We introduce a progressive autoregressive distillation pipeline to transform a large bidirectional audio-

video diffusion model into a few-step causal generator; a synchronized audio-video long-short-term memory to preserve long-duration consistency and cross-modal alignment under a bounded memory budget; and a hierarchical rolling prompt planning strategy to enable coherent semantic evolution and seamless prompt transitions under the rolling-forcing setting. Extensive experiments demonstrate that Omni-LiveAvatar achieves a 33× speedup over its LTX-2 teacher on a single NVIDIA H200 GPU while outperforming real-time baselines across all evaluated metrics.

References

Chen, Y.; Liang, S.; Zhou, Z.; Huang, Z.; Ma, Y.; Tang, J.; Lin, Q.; Zhou, Y.; and Lu, Q. 2025. HunyuanVideo-Avatar: High-Fidelity Audio-Driven Human Animation for Multiple Characters. arXiv:2505.20156.

Chen, Z.; Cao, J.; Chen, Z.; Li, Y.; and Ma, C. 2024. EchoMimic: Lifelike Audio-Driven Portrait Animations through Editable Landmark Conditions. arXiv:2407.08136.

Chung, J. S.; and Zisserman, A. 2016. Out of time: automated lip sync in the wild. In *Asian conference on computer vision*, 251–263. Springer.

Cui, J.; Li, H.; Yao, Y.; Zhu, H.; Shang, H.; Cheng, K.; Zhou, H.; Zhu, S.; and Wang, J. 2024. Hallo2: Long-Duration and High-Resolution Audio-Driven Portrait Image Animation. arXiv:2410.07718.

Cui, J.; Li, H.; Zhan, Y.; Shang, H.; Cheng, K.; Ma, Y.; Mu, S.; Zhou, H.; Wang, J.; and Zhu, S. 2025. Hallo3: Highly Dynamic and Realistic Portrait Image Animation with Video Diffusion Transformer. arXiv:2412.00733.

Ge, X.; Zhang, X.; Xu, T.; Zhang, Y.; Zhang, X.; Wang, Y.; and Zhang, J. 2026a. SenseFlow: Scaling Distribution Matching for Flow-based Text-to-Image Distillation. arXiv:2506.00523.

Ge, X.; Zhang, Y.; Huang, Y.; He, D.; Wang, X.; Ma, B.; Song, G.; Liu, Y.; and Zhang, J. 2026b. Salt: Self-Consistent Distribution Matching with Cache-Aware Training for Fast Video Generation. arXiv:2604.03118.

HaCohen, Y.; Brazowski, B.; Chiprut, N.; Bitterman, Y.; Kvochko, A.; Berkowitz, A.; Shalem, D.; Lifschitz, D.; Moshe, D.; Porat, E.; Richardson, E.; Shiran, G.; Chachy, I.; Chetboun, J.; Finkelson, M.; Kupchick, M.; Zabari, N.; Guetta, N.; Kotler, N.; Bibi, O.; Gordon, O.; Panet, P.; Benita, R.; Armon, S.; Kulikov, V.; Inger, Y.; Shiftan, Y.; Melumian, Z.; and Farbman, Z. 2026. LTX-2: Efficient Joint Audio-Visual Foundation Model. arXiv:2601.03233.

Huang, X.; Li, Z.; He, G.; Zhou, M.; and Shechtman, E. 2025. Self Forcing: Bridging the Train-Test Gap in Autoregressive Video Diffusion. arXiv:2506.08009.

Huang, Y.; Ge, X.; Gong, R.; Lv, C.; and Zhang, J. 2026a. LinVideo: A Post-Training Framework towards O(n) Attention in Efficient Video Generation. arXiv:2510.08318.

Huang, Y.; Gong, R.; Liu, J.; Ding, Y.; Lv, C.; Qin, H.; and Zhang, J. 2026b. QVGen: Pushing the Limit of Quantized Video Generative Models. arXiv:2505.11497.

Huang, Y.; Guo, H.; Wu, F.; Wang, W.; Zhang, S.; Huang, S.; Gan, Q.; Liu, L.; Zhao, S.; Chen, E.; Liu, J.; and Hoi, S. 2026c. Live Avatar: Streaming Real-time Audio-Driven Avatar Generation with Infinite Length. arXiv:2512.04677.

Huang, Z.; He, Y.; Yu, J.; Zhang, F.; Si, C.; Jiang, Y.; Zhang, Y.; Wu, T.; Jin, Q.; Chanpaisit, N.; Wang, Y.; Chen, X.; Wang, L.; Lin, D.; Qiao, Y.; and Liu, Z. 2023. VBench: Comprehensive Benchmark Suite for Video Generative Models. arXiv:2311.17982.

Huang, Z.; Zhang, F.; Xu, X.; He, Y.; Yu, J.; Dong, Z.; Ma, Q.; Chanpaisit, N.; Si, C.; Jiang, Y.; Wang, Y.; Chen, X.; Chen, Y.-C.; Wang, L.; Lin, D.; Qiao, Y.; and Liu, Z. 2024. VBench++: Comprehensive and Versatile Benchmark Suite for Video Generative Models. arXiv:2411.13503.

Jiang, J.; Liang, C.; Yang, J.; Lin, G.; Zhong, T.; and Zheng, Y. 2025. Loopy: Taming Audio-Driven Portrait Avatar with Long-Term Motion Dependency. arXiv:2409.02634.

Kong, W.; Tian, Q.; Zhang, Z.; Min, R.; Dai, Z.; Zhou, J.; Xiong, J.; Li, X.; Wu, B.; Zhang, J.; et al. 2024. Hunyuanvideo: A systematic framework for large video generative models. *arXiv preprint arXiv:2412.03603*.

Li, C.; Li, J.; Mei, R.; Xia, H.; Zhu, H.; Wang, J.; and Zhu, S. 2026. Hallo-Live: Real-Time Streaming Joint Audio-Video Avatar Generation with Asynchronous Dual-Stream and Human-Centric Preference Distillation. arXiv:2604.23632.

Li, Y.; Liu, Z.; Li, Z.; Lin, Z.; and Zhang, J. 2025. RemedyGS: Defend 3D Gaussian Splatting against Computation Cost Attacks. arXiv:2511.22147.

Lin, F.; Hu, Y.; Zhu, L.; Liu, Z.; Huang, Y.; Lin, Z.; and Zhang, J. 2026. Real-Time Human Frontal View Synthesis from a Single Image. arXiv:2603.15433.

Liu, J.; Liu, G.; Liang, J.; Yuan, Z.; Liu, X.; Zheng, M.; Wu, X.; Wang, Q.; Xia, M.; Wang, X.; Liu, X.; Yang, F.; Wan, P.; Zhang, D.; Gai, K.; Yang, Y.; and Ouyang, W. 2025a. Improving Video Generation with Human Feedback. arXiv:2501.13918.

Liu, K.; Hu, W.; Xu, J.; Shan, Y.; and Lu, S. 2025b. Rolling Forcing: Autoregressive Long Video Diffusion in Real Time. arXiv:2509.25161.

Low, C.; Wang, W.; and Katyal, C. 2025. Ovi: Twin Backbone Cross-Modal Fusion for Audio-Video Generation. arXiv:2510.01284.

McAuliffe, M.; Socolof, M.; Mihuc, S.; Wagner, M.; and Sonderegger, M. 2017. Montreal Forced Aligner: Trainable Text-Speech Alignment Using Kaldi. In *Interspeech 2017*, 498–502.

Mittag, G.; Naderi, B.; Chehadi, A.; and Möller, S. 2021. NISQA: A Deep CNN-Self-Attention Model for Multidimensional Speech Quality Prediction with Crowdsourced Datasets. In *Interspeech 2021*, 2127–2131.

Radford, A.; Kim, J. W.; Xu, T.; Brockman, G.; McLeavey, C.; and Sutskever, I. 2022. Robust Speech Recognition via Large-Scale Weak Supervision. arXiv:2212.04356.

Reddy, C. K. A.; Gopal, V.; and Cutler, R. 2022. DNSMOS P.835: A Non-Intrusive Perceptual Objective Speech Quality Metric to Evaluate Noise Suppressors. arXiv:2110.01763.

Ruan, L.; Ma, Y.; Yang, H.; He, H.; Liu, B.; Fu, J.; Yuan, N. J.; Jin, Q.; and Guo, B. 2023. MM-Diffusion: Learning Multi-Modal Diffusion Models for Joint Audio and Video Generation. arXiv:2212.09478.

Saeki, T.; Xin, D.; Nakata, W.; Koriyama, T.; Takamichi, S.; and Saruwatari, H. 2022. UTMOS: UTokyo-SaruLab System for VoiceMOS Challenge 2022. arXiv:2204.02152.

Shen, L.; Qiao, Q.; Yu, T.; Zhou, K.; Yu, T.; Zhan, Y.; Wang, Z.; Tao, M.; Yin, S.; and Liu, S. 2025. SoulX-FlashTalk: Real-Time Infinite Streaming of Audio-Driven Avatars via Self-Correcting Bidirectional Distillation. arXiv:2512.23379.

SII-GAIR; ai, S.; Chern, E.; Teng, H.; Sun, H.; Wang, H.; Pan, H.; Jia, H.; Su, J.; Li, J.; Yu, J.; Liu, L.; Li, L.; Ye, L.; Hu, M.; Wang, Q.; Qi, Q.; Chern, S.; Bu, T.; Wang, T.; Xu, T.; Zhang, T.; Mi, T.; Xu, W.; Zhang, W.; Zhang, W.; Yi, X.; Cai, X.; Kang, X.; Ma, Y.; Liu, Y.; Zhang, Y.; Huang, Y.; Lin, Y.; Tao, Z.; Liu, Z.; Zhang, Z.; Cen, Z.; Yu, Z.; Wang, Z.; Hu, Z.; Zhou, Z.; Guo, Z.; Cao, Y.; and Liu, P. 2026. Speed by Simplicity: A Single-Stream Architecture for Fast Audio-Video Generative Foundation Model. *arXiv preprint arXiv:2603.21986*.

Su, Y.; Li, Y.; Xue, Z.; Huang, J.; Fu, S.; Li, H.; Li, Y.; Qian, Z.; Huang, H.; and Duan, N. 2026. OmniForcing: Unleashing Real-time Joint Audio-Visual Generation. arXiv:2603.11647.

Tian, L.; Wang, Q.; Zhang, B.; and Bo, L. 2024. EMO: Emote Portrait Alive – Generating Expressive Portrait Videos with Audio2Video Diffusion Model under Weak Conditions. arXiv:2402.17485.

Tu, S.; Pan, Y.; Huang, Y.; Han, X.; Xing, Z.; Dai, Q.; Luo, C.; Wu, Z.; and Jiang, Y.-G. 2025. StableAvatar: Infinite-Length Audio-Driven Avatar Video Generation. arXiv:2508.08248.

Wan, T.; Wang, A.; Ai, B.; Wen, B.; Mao, C.; Xie, C.-W.; Chen, D.; Yu, F.; Zhao, H.; Yang, J.; Zeng, J.; Wang, J.; Zhang, J.; Zhou, J.; Wang, J.; Chen, J.; Zhu, K.; Zhao, K.; Yan, K.; Huang, L.; Feng, M.; Zhang, N.; Li, P.; Wu, P.; Chu, R.; Feng, R.; Zhang, S.; Sun, S.; Fang, T.; Wang, T.; Gui, T.; Weng, T.; Shen, T.; Lin, W.; Wang, W.; Wang, W.; Zhou, W.; Wang, W.; Shen, W.; Yu, W.; Shi, X.; Huang, X.; Xu, X.; Kou, Y.; Lv, Y.; Li, Y.; Liu, Y.; Wang, Y.; Zhang, Y.; Huang, Y.; Li, Y.; Wu, Y.; Liu, Y.; Pan, Y.; Zheng, Y.; Hong, Y.; Shi, Y.; Feng, Y.; Jiang, Z.; Han, Z.; Wu, Z.-F.; and Liu, Z. 2025. Wan: Open and Advanced Large-Scale Video Generative Models. arXiv:2503.20314.

Xu, M.; Li, H.; Su, Q.; Shang, H.; Zhang, L.; Liu, C.; Wang, J.; Yao, Y.; and Zhu, S. 2024a. Hallo: Hierarchical Audio-Driven Visual Synthesis for Portrait Image Animation. arXiv:2406.08801.

Xu, S.; Chen, G.; Guo, Y.-X.; Yang, J.; Li, C.; Zang, Z.; Zhang, Y.; Tong, X.; and Guo, B. 2024b. VASA-1: Lifelike Audio-Driven Talking Faces Generated in Real Time. arXiv:2404.10667.

Yang, S.; Huang, W.; Chu, R.; Xiao, Y.; Zhao, Y.; Wang, X.; Li, M.; Xie, E.; Chen, Y.; Lu, Y.; Han, S.; and Chen, Y. 2025a. LongLive: Real-time Interactive Long Video Generation. arXiv:2509.22622.

Yang, S.; Kong, Z.; Gao, F.; Cheng, M.; Liu, X.; Zhang, Y.; Kang, Z.; Luo, W.; Cai, X.; He, R.; and Wei, X. 2025b. InfiniteTalk: Audio-driven Video Generation for Sparse-Frame Video Dubbing. arXiv:2508.14033.

Yin, T.; Gharbi, M.; Zhang, R.; Shechtman, E.; Durand, F.; Freeman, W. T.; and Park, T. 2024. One-step Diffusion with Distribution Matching Distillation. arXiv:2311.18828.

Yin, T.; Zhang, Q.; Zhang, R.; Freeman, W. T.; Durand, F.; Shechtman, E.; and Huang, X. 2025. From Slow Bidirectional to Fast Autoregressive Video Diffusion Models. arXiv:2412.07772.

Zhao, J.; Wei, F.; Liu, Z.; Zhang, H.; Xu, C.; and Lu, Y. 2025. Spatia: Video Generation with Updatable Spatial Memory. arXiv:2512.15716.

Zhen, D.; Yin, S.; Qin, S.; Yi, H.; Zhang, Z.; Liu, S.; Qi, G.; and Tao, M. 2025. Teller: Real-Time Streaming Audio-Driven Portrait Animation with Autoregressive Motion Generation. arXiv:2503.18429.

Zheng, D.; Huang, Z.; Liu, H.; Zou, K.; He, Y.; Zhang, F.; Gu, L.; Zhang, Y.; He, J.; Zheng, W.-S.; Qiao, Y.; and Liu, Z. 2025. VBench-2.0: Advancing Video Generation Benchmark Suite for Intrinsic Faithfulness. arXiv:2503.21755.

Zhu, L.; Huang, Y.; Ge, X.; Xue, Y.; Liu, Z.; Zhang, Y.; Lin, Z.; and Zhang, J. 2026. Flash-VAED: Plug-and-Play VAE Decoders for Efficient Video Generation. arXiv:2602.19161.

Additional Qualitative Comparisons on 60-Second Avatar Generation

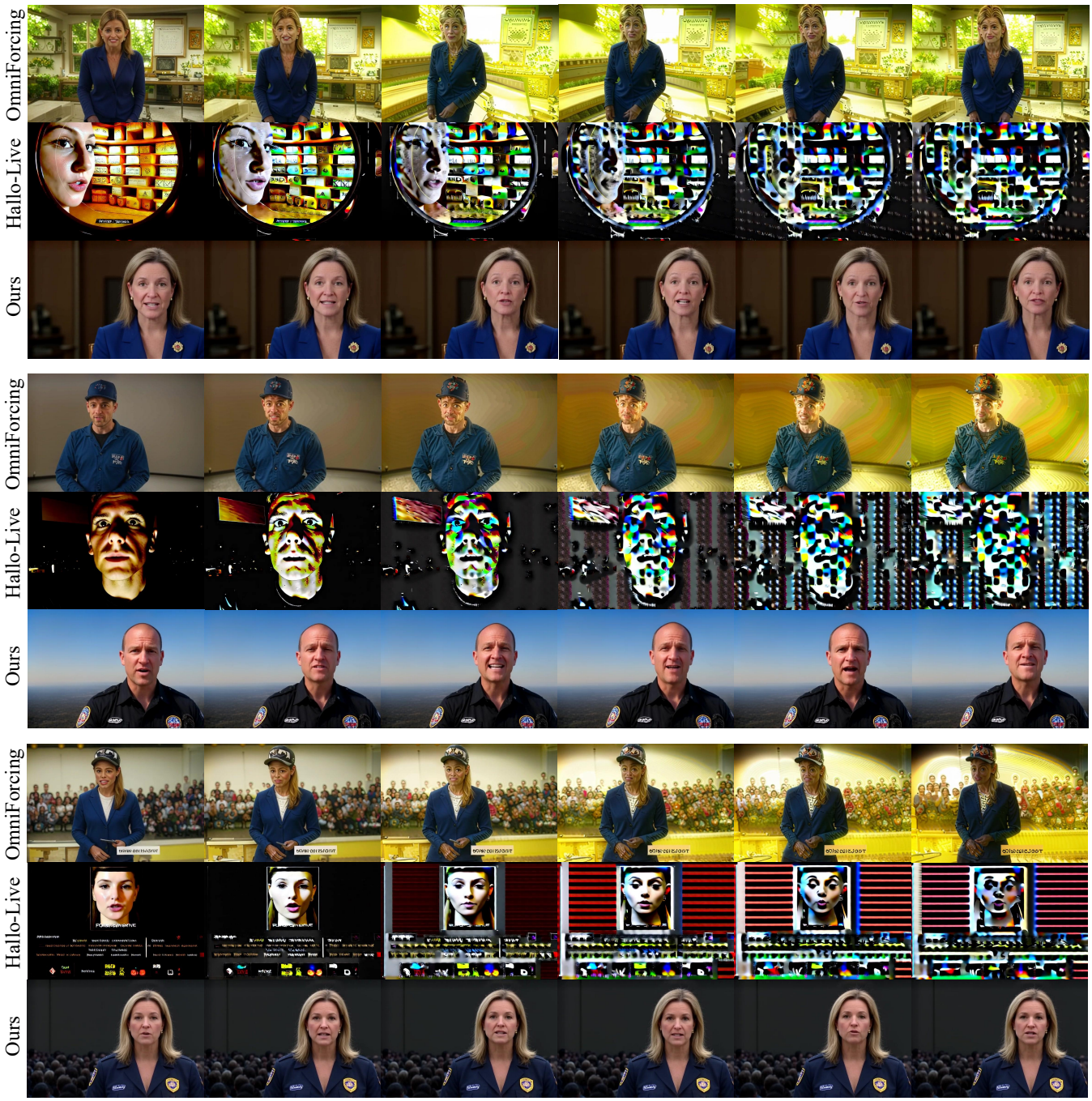

Figure 5: Additional qualitative comparisons on 60-second avatar generation. Omni-LiveAvatar maintains consistent avatar and background appearance and accurate audio-video synchronization throughout minute-long generation.

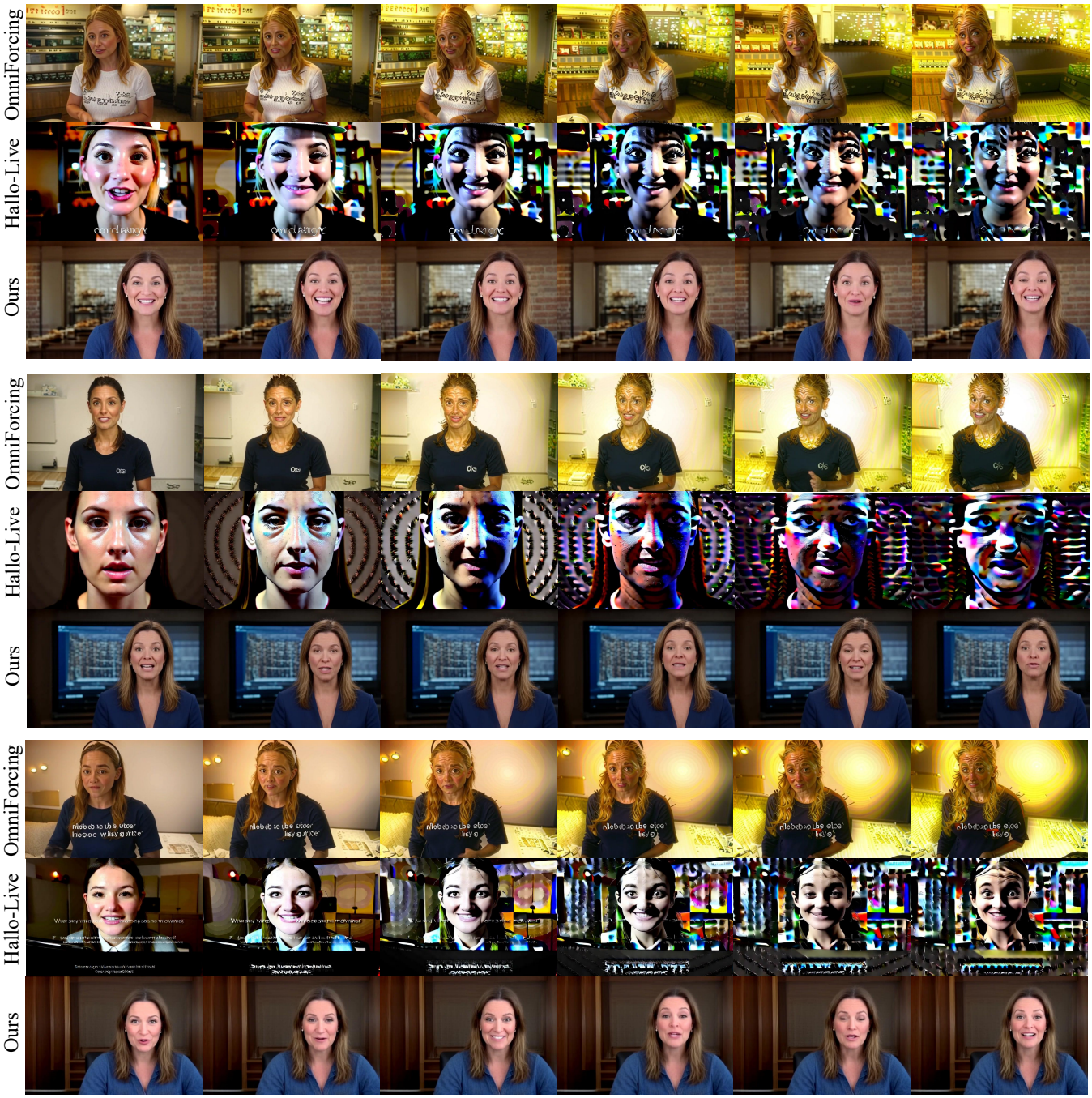

Figure 5 (continued).